

***Chapter III***  
***Materials and Methods***

## Chapter III

### MATERIALS AND METHODS

#### 3.1 Materials

The present research required various materials ranging from many equipment to chemicals and reagents, and few software tools and computer applications. The various equipments and materials used in the present research are listed in Table 3.1

#### 3.2 Methods

The overall methodology of the present work is represented in a flow chart shown below. The entire work comprised of five objectives, starting with the design and development of an OH setup followed by the characterization of mango puree. Further, the OH conditions were optimized on the basis of responses viz., enzyme and microbial inactivation and change in the color of the product. The kinetics of the change in the responses was the aim of the next objective; finally, the process optimized OH condition was compared with conventional heating for the immediate effects on various parameters of mango puree and also its storage study.

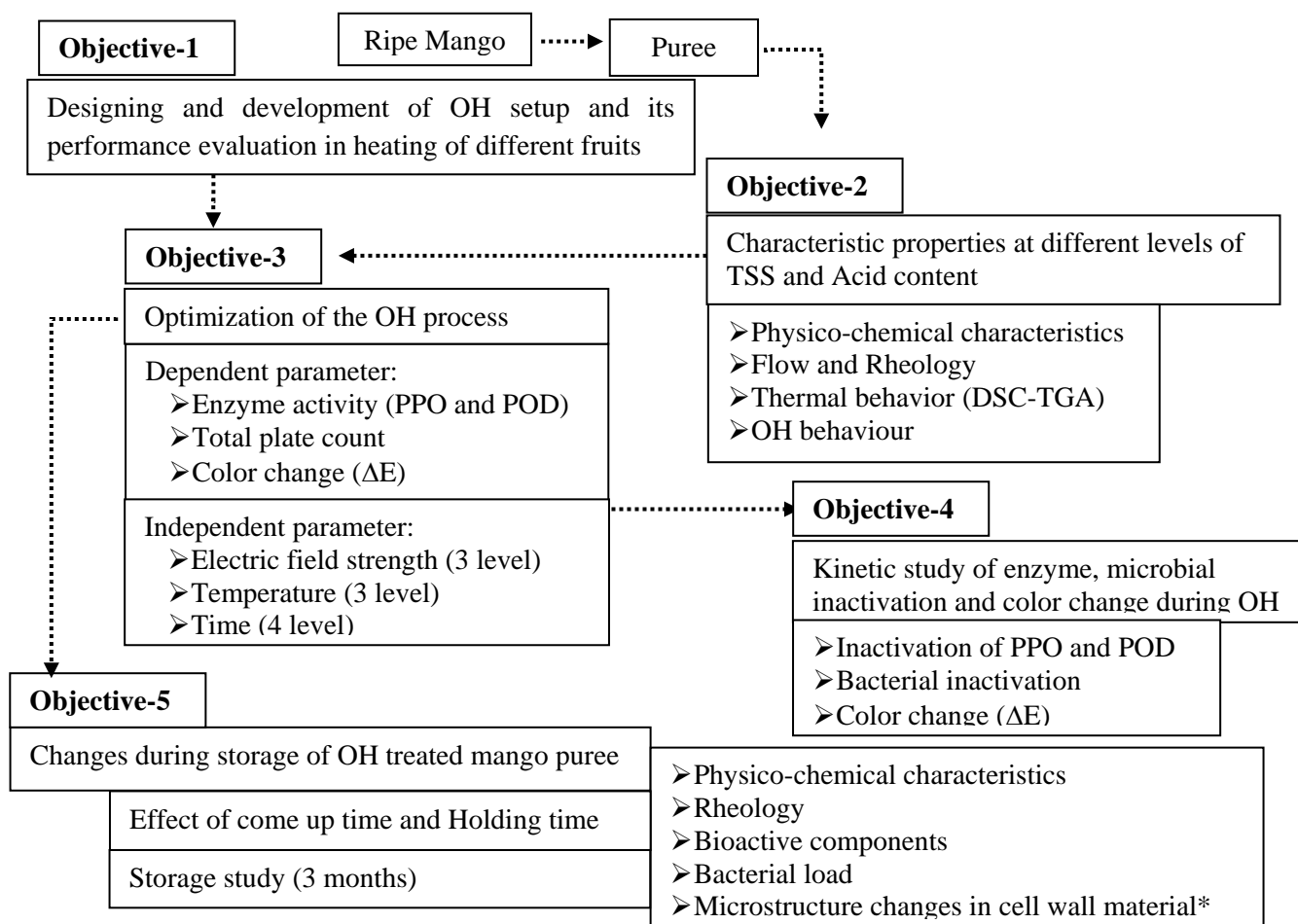


Table 3.1 The details of materials required in the present research

	Ohmic heating setup	Food samples	Equipments	Chemicals/Reagents	Software
Materials	Data logger	Litchi juice	Centrifuge	2, 6 Dichloroindophenol	Design Expert 7.1
	Electricity supply	Mango puree	Differential Scanning Calorimeter	Acetone	Microsoft Office7
	Platinized-titanium electrodes	Pineapple juice	Thermo Gravimetric Analyzer	Catechol	OriginPro.85
	Teflon chamber	Tomato juice	Distillation unit	Citric acid	SPSS.16
	Variac transformer	Watermelon juice	Food processor	Double Distilled Water	
			Hand Blender	Folin-Ciocalteu's	
			Hot Water bath	Reagent	
			Incubation Shaker	Gallic Acid	
			pH meter	Glucose	
			Refractometer	Guaicol	
			Rheometer	Hexane	
			Spectro-photometer	Hydrogen Peroxide	
			Scanning Electron Microscope	Meta-Phosphoric Aci	
			Texture analyzer	Peptone Water	
			Ultra-Scan VIS, Hunter Lab	Plate Count Agar	
			Vacuum Oven	Sodium Carbonate	
		vortex shaker	Sodium Hydroxide		
		Water activity meter	Sodium Phosphate Buffer		

### **3.2.1 Design and development of Ohmic heating (OH) Setup**

#### **3.2.1.1 Design requirements**

The OH setup must fulfill the following design requirements:

1. The setup should have a holding volume of 50 mL of liquid food in a batch operation.
2. The heating cell should not be an electric conductor and heat conductor to avoid the chance of short circuit and heat loss.
3. The electrodes should be resistant to corrosive reaction with liquid food.
4. The system must be capable of maintaining varying electric field across the electrodes.
5. The system must be capable of temperature control at set point.
6. The system must be capable of microprocessor based online data acquisition of different variables viz., applied voltage, current and temperature at regular intervals.
7. The system should be portable in nature so that it can be accommodated in the laboratory.
8. The set-up should be compatible with 220V, 50 Hz Indian system.
9. The system must have an easy drainage facility for discharge of processed liquid food.
10. The system must be easy to clean after dismantling of the component.

#### **3.2.1.2 Conceptual design**

The ohmic heating (OH) system was designed with an aim so that an electrically conductive food material can be heated by the joules heating concept. The setup should be comprised of a space in between two electrodes, and supply of electric voltage to be applied across the electrodes. The food material in between the electrodes gets heated once the electrical current gets induced due to applied electric voltage and the resistance to the induced current results in the increase in the temperature following the joules law of heating. The electric voltage could be controlled by the variac transformer to set the desired electric field strength without changing the distance between the electrodes. The temperature could be controlled by simply stopping the electric voltage supply with the help of a relay based temperature controller. The data of temperature, voltage and current can be recorded by putting the data logger in place during the heating process. The schematic diagram of the design is illustrated in Fig. 3.1.

### 3.2.1.3 Design and fabrication ohmic heating setup

Based on the conceptual design, a lab scale OH setup was developed. The lab scale ohmic heating assembly comprised of the following components:

- (i) Heating chamber
- (ii) Electrodes
- (iii) Power supply and voltage control
- (iv) Microprocessor based data acquisitioning assembly

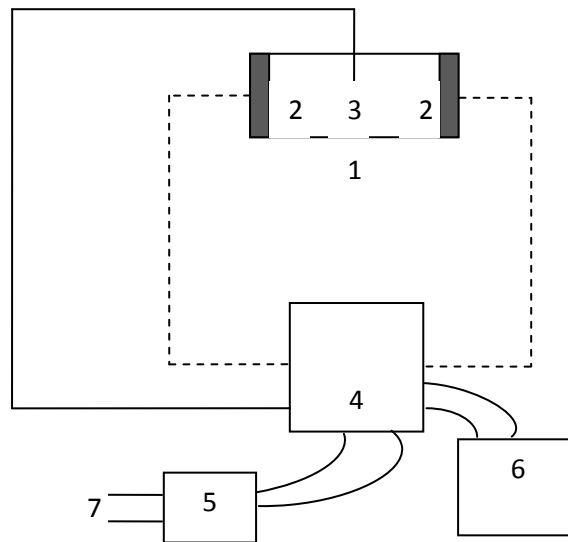


**Fig. 3.1 Ohmic heating setup conceptual design comprised of heating chamber (1), electrodes (2), temperature controller (3), data acquisitioning assembly (4), variac transformer (5), computer (6) and electric power supply (7)**

### 3.2.1.4 Heating chamber

The heating chamber was fabricated in same line as that reported by Olivera et al. [22] and Darvishi et al. [9] with some modifications. Teflon material is reported to be a good insulating material for current and heat, and it is extensively used in many industries [21]. Hence, it was selected to fabricate the main heating chamber for ohmic heating purpose. The heating chamber was cylindrical in shape with 25.4, 50 and 120 mm internal diameter, external diameter and length respectively. The specifications of heating chamber are presented in Table 3.2, and its schematic diagram is shown in Fig. 3.2, and the actual chamber is shown in Fig. 3.3. To fasten the electrodes on either side of hollow opening of the chamber, two detachable lids were provided. The lids get easily fastened at both the ends with spiral thread joints over the length of 10 mm from either end. Thus, the actual length of heating chamber for sample was 100 mm. The heating chamber was fabricated in the Central workshop, Tezpur University. The heating chamber was tested

for leakage through the joints and it was made leak proof. The capacity of the heating chamber was around  $50\pm 0.5$  ml. Provisions were made for the easy dismantling of the heating chamber for cleaning of cylindrical chamber or electrodes.

Three apertures of 3-mm diameter were made on the surface at the centre (50 mm from ends of the chamber) and at a distance of 25 mm on either side of the central aperture. The purpose of these apertures was to inject the sample into the chamber and to measure the temperature during heating. The temperature controlling thermocouple was inserted through the aperture located at the centre and kept at the geometrical centre of the sample.

**Table 3.2 Specification of Teflon heating chamber of ohmic heating**

Specification	Unit	Value
Density	$\text{g/cm}^3$	$2.20\pm 0.02$
Diameter (in)	mm	$25.54\pm 0.01$
Diameter (out)	mm	$50.00\pm 0.01$
Length	mm	$100.00\pm 0.01$
Volume (solid Teflon)	$\text{cm}^3$	$145.17\pm 0.20$
Volume (hollow space)	$\text{cm}^3$	$50.64\pm 0.20$
Mass of chamber	kg	$0.319\pm 0.002$
Specific heat ( $C_p$ )	$\text{kJ/kg}^\circ\text{C}$	$0.97\pm 0.01$
$m\times C_p$	$\text{kJ}^\circ\text{C}$	$0.310\pm 0.005$

Note: the specific heat was measured from [21]

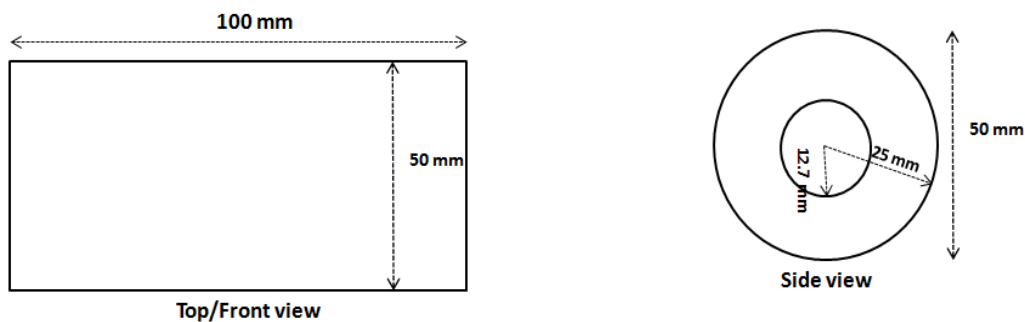


**Fig. 3.2 Dimensions of the hollow cylindrical Teflon heating chamber**

### 3.2.1.5 Electrodes

The researchers in the past have reported that there are chances of metal ion transfer from the electrode to the food material due to electrophoresis [23, 25]. Thus, a suitable electrode needs to be selected to avoid such unwanted metal ion transfer into the food during ohmic heating. Samaranayake and Sastry [25] found that the platinized titanium

electrodes restrict the chances of corrosion during OH process. Thus, circular electrodes (radius of 25.6 mm and 1 mm thickness) made of titanium as base material with a 2.5-micron plating of platinum as shown in Fig. 3.3 (c), were used in the present study. The electrodes were manufactured and supplied by TI-Anode Fabricators Pvt. Ltd, Chennai, India.

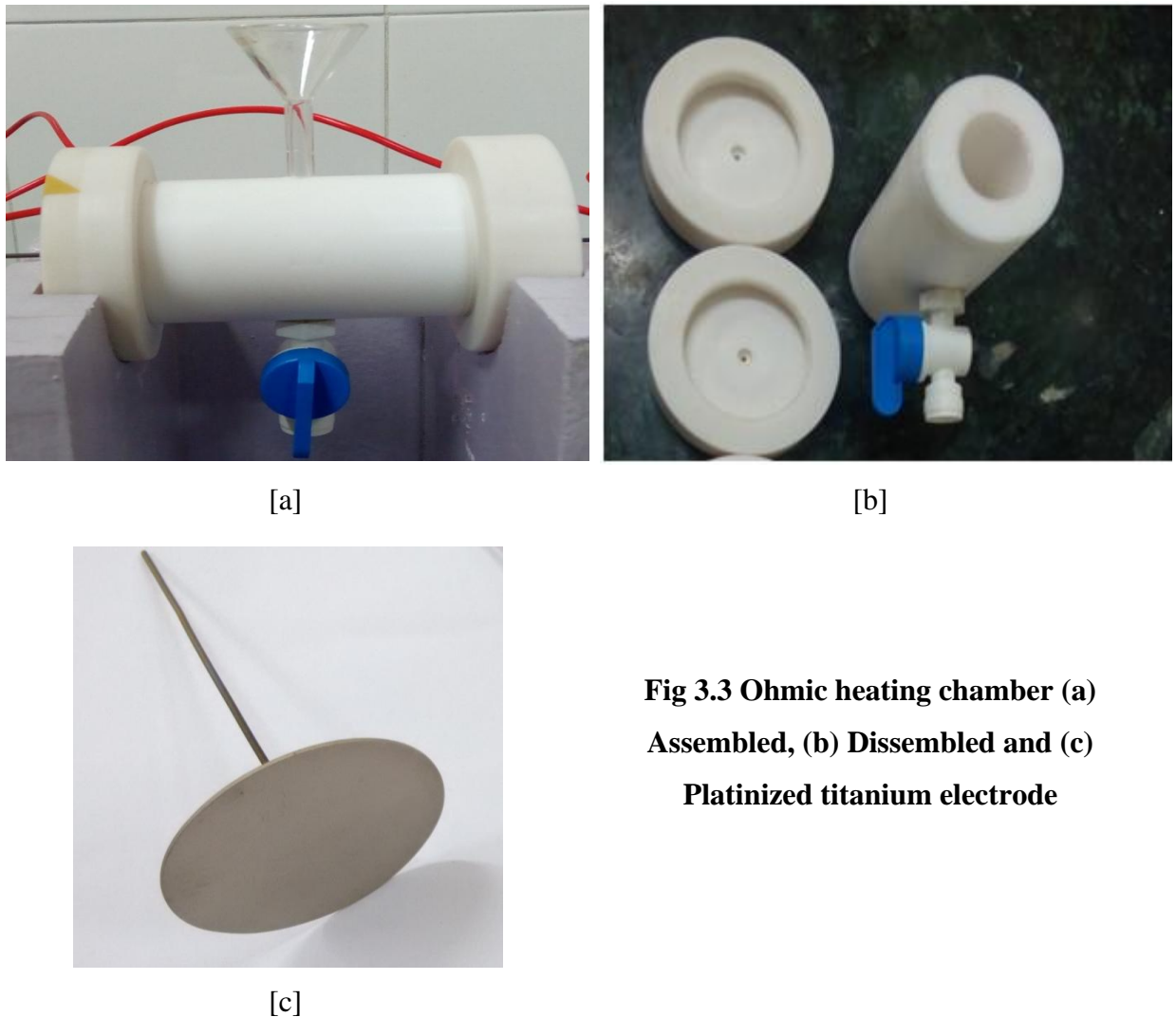


**Fig 3.3 Ohmic heating chamber (a) Assembled, (b) Dissembled and (c) Platinized titanium electrode**

### 3.2.1.6 Power supply and voltage control

Domestic electrical power supply of 240 V, single phase ( $\Phi$ ) and 50 Hz was supplied to the electrodes of the ohmic heating assembly. The amount of voltage to be supplied to the food material via electrodes was controlled by variac transformer. The variac transformer was procured from Servo Star India Pvt Ltd., Delhi, India. The specification of the variac transformer was single phase with output voltage range of 0-

400 V and current capacity of 5 amps. Therefore, the deigned OH system has the working range capacity of 0-40 V/cm Electric Field Strength (EFS).

### **3.2.1.7 Microprocessor based data acquisitioning assembly**

Multi-channel (8 channels) data logger with one voltage, one current and four temperature transducers (six busy and two blank channels) was designed by the research group and finally assembled and developed by Research and Design Laboratories, Bangalore India. The temperature at different locations, voltage and current flowing through the sample during the OH process was measured by the sensors attached to the respective transducer. One of the temperature sensors (K-type thermocouple) was connected with relay based inbuilt in temperature controller in microprocessor and was employed for controlling the temperature. The temperature was controlled by breaking the circuit or cutting down the power supply once the desired temperature was achieved.

### **3.2.2 Samples for performance evaluation**

Five different season fruits were selected on the base of availability in different seasons. The selected fruits for performance evaluation of OH setup are listed in Table 3.3. The fresh, fully ripe free from any damage fruits were collected from a local market near Tezpur, India. The fruits were properly washed and cleaned with water for any external dirt instantly after bringing them to the laboratory.

### **3.2.3 Sample preparation**

The fruits were peeled/ pulped/ deseeded manually using stainless steel knives carefully to check the microbial contamination by using sterilized gloves and glass ware. Domestic food processor (USHA, MODEL–FP2663, India) was used to prepare juice or puree out of the fruit pieces or pulp respectively. The juice of tomato, watermelon, pineapple and litchi was extracted by passing the crushed pulp through the double layered muslin cloth, where as the mango puree was prepared by blending the fresh pulp for almost 2 min. The fresh juice/puree was analyzed for various physico-chemical parameters such as moisture content, total soluble solids (TSS), acidity and pH (methodology discussed ahead).



**Table 3.3 The list of food materials analyzed for performance of OH process**

S. No.	Material	Variety
1.	Mango ( <i>Mangifera indica</i> ) puree	<i>Chausa</i>
2.	Tomato ( <i>Lycopersicon esculentu</i> ) juice	<i>Rupali</i>
3.	Watermelon ( <i>Citrullus vulgaris</i> ) juice	<i>Hybrid</i>
4.	Pineapple ( <i>Ananas cosmosus</i> ) juice	<i>Hybrid</i>
5.	Litchi ( <i>Litchi chinensis</i> ) juice	<i>Piyazi</i>

### 3.2.4 Properties of the sample

The juice or puree of different fruits was analyzed for the following parameters:

#### 3.2.4.1 Moisture content

The moisture of the samples was determined by following the method of Icier et al. [15] with some modifications, the moisture was removed by drying the samples using vacuum oven (OV-11, JEIOTech, Korea) at a vacuum of 560 mmHg and temperature of 60 °C for 24 hours or until no change in consecutive reading of sample weight. The moisture content is expressed on wet basis and was calculated by the following equation (Eq. 3.1).

$$\text{Moisture content (\%)} = \frac{(W_i - W_e) - (W_f - W_e)}{(W_i - W_e)} \times 100 \quad \text{Eq. (3.1)}$$

Where:

$W_i$  is the initial weight (g) of the dish with sample,

$W_e$  is the weight (g) of the empty dish,

$W_f$  is the weight (g) of the dish with sample after drying

#### 3.2.4.2 Density

Density was measured with standard procedure using 25 mL pycnometer (Borosil) by Eq. 3.2 Using distilled water as the reference material; the density was measure at room temperature.

$$\text{Density} = \frac{m_f - m_e}{v_p} \quad \text{Eq. (3.2)}$$

Where  $m_f$  and  $m_e$  is mass of sample filled and empty pyknometer, and  $v_p$  is volume of the pyknometer (25 mL or cubic cm).

#### 3.2.4.3 Total soluble solids (TSS)

Total soluble solids were measured with the help of a hand refractometer (Erma Tokyo, Japan), calibrated with double distilled water before the measurement.

### 3.2.4.4 Titratable acidity

Standard titration procedure was used to measure the titratable acidity of the samples. The samples were titrated with 0.01 N NaOH solution using phenolphthalein as indicator, the acidity was calculated by using the Eq. 3.3.

$$\text{Titratable acidity (\%)} = \frac{\text{Titre value} \times \text{Normality (NaOH)} \times \text{Volume makeup} \times 64 \times 100}{\text{Volume of aliquot} \times \text{Volume of sample} \times 1000} \times 100 \quad \text{Eq. (3.3)}$$

### 3.2.4.5 pH

The pH of the samples was measured by using a pH meter (Eutech Instruments, pH 510), the instrument was calibrated with standard buffer of pH 4.0, 7.0 and 9.1 before taking the sample reading, the measurements were carried at room temperature.

### 3.2.5 Performance evaluation OH process

The performance of the designed OH setup was evaluated on the base of percentage of electrical energy utilized to heat the food material at particular EFS. The different selected samples were heated from room temperature up to 90 °C at electric field strength (EFS) of 10, 20, 30 and 40 V.cm<sup>-1</sup> in the OH setup. The heating rate and electrical conductivity was calculated from the data collected (Temperature, Current and Voltage) by the data acquisitioning system. The data collected was utilized for the performance evaluation of OH process of various food materials at the above mentioned EFS range. Following are the parameters determined for the e performance evaluation of the designed OH setup.

#### 3.2.5.1 Electrical conductivity

The electrical conductivity of the sample was calculated from the dimensions of the heating chamber (length and area) and voltage and ampere data collected by the data logger using the following equation Eq. 3.4 [20, 26].

$$\sigma = \frac{L}{A} \times \frac{I}{V} \quad \text{Eq. (3.4)}$$

Electric conductivity of a material has a linear relation with its temperature; it increases with increasing the temperature (generally linearly). The constant of the dependent electric filed is calculated by the following Eq. 3.5 using linear regression analysis [20].

$$\sigma_T = \sigma_i + mT \quad \text{Eq. (3.5)}$$

Where ' $\sigma_T$ ' and ' $\sigma_i$ ' is the electrical conductivity at temperature T ( $^{\circ}\text{C}$ ) and electrical conductivity at reference temperature, ' $m$ ' is temperature constant of EC.

### 3.2.5.2 Heat capacity (Specific heat, $C_p$ )

The heat capacity of the samples was estimated by using the following expression Eq. 3.6 [11].

$$C_p = 1.675 + (0.025 \times mc) \quad \text{Eq. (3.6)}$$

Where mc is the moisture content (wet basis) of sample.

### 3.2.5.3 Heating rate

The actual amount of energy required to heat the samples from room temperature to  $90^{\circ}\text{C}$  was calculated by the Eq. 3.7 [10] whereas the mass of the sample was calculated by the Eq. 3.8.

$$Q = mC_p(T_f - T_i) \quad \text{Eq. (3.7)}$$

$$m = \rho \times V \quad \text{Eq. (3.8)}$$

Where  $\rho$  is Density ( $\text{g}/\text{cm}^3$ ) and ' $V$ ' is, Volume of the heating chamber ( $\text{cm}^3$ )

### 3.2.5.4 Heating power

The power of the heating during OH at different EFS was calculated from the voltage and current data collected during the experiment and using the Eq. 3.9 [13].

$$P = \Sigma VI\Delta t \quad \text{Eq. (3.9)}$$

### 3.2.5.5 Energy efficiency

The energy efficiency was calculated considering the heat capacity at initial and final temperature and also assuming that 99 % of electrical power gets utilized for energy generation energy, therefore the energy efficiency of the OH process of the different samples was calculated by Eq. 3.10 as suggested by Bozkurt and Icier [5].

$$\text{Energy efficiency (\%)} = \frac{m (C_p \times T_f)}{m (C_p \times T_i) + Q_s} \times 100 \quad \text{Eq. (3.10)}$$

$$Q_s = 0.99 \times P \quad \text{Eq. (3.11)}$$

### 3.2.5.6 Heat loss into the heating chamber

The loss of the heat was calculated form Eq. 3.12.

$$\text{Heat loss} = mC_p(T_f - T_i) = V_{Tf} \times \sigma_{Tf} \times C_p(T_f - T_i) \quad \text{Eq. (3.12)}$$

Where,

- $C_p$  is the specific heat of teflon  
 $T_f$  is the average of surface and final sample temperature  
 $T_i$  is the initial temperature of heating cell (RT)  
 $V_{tf}$  is volume of solid heating chamber  
 $\sigma_{Tf}$  is density of the Teflon

$$V_{Tf} = \text{Volume of the solid teflon} = L\pi(R_o^2 - R_i^2) \quad \text{Eq. (3.13)}$$

Where,

$R_o$ ,  $R_i$  and  $L$  are outer radius, inner radius and length of the heating chamber, respectively.

In the present study the energy other than the energy utilized for heating sample and heating the OH chamber was assumed to get wasted in atmosphere from the surface of the heating chamber, or involved in some electrochemical reactions within the material [14].

### 3.2.6 Mango puree characterization on the basis of Acid and TSS content

Mango purees is relatively viscous and thick in consistency to its juice or nectar counterpart and its uneasy to make its thin film for rapid and uniform heat transfer by conduction heating method. Therefore, it is difficult to process mango puree by the application of conventional thermal processing method. India is the largest producer of mango and to the best knowledge of research team; very limited literature is reported on OH process of mango puree as such. Hence mango puree was selected for the study in detail next onwards in the present study.

#### 3.2.6.1 Sample preparation

The fresh and fully ripe mangoes (*Mangifera indica*) of ‘‘Chausa variety’’ were purchased from the local market (Tezpur India). The fruits were thoroughly washed with water and the adhered water was wiped followed by drying of the surface moisture at room temperature immediately after the mangoes were brought to the research laboratory. Healthy and undamaged fruits were chosen for the preparation of the puree. The fruits were peeled, deseeded, and the pulp obtained was blended for 2 min using a household hand blender (Orpat HHB-107E (WOB), India) with ribbon-shaped blades until a homogeneous puree was obtained. The total soluble solids (TSS) and acid content) of the puree were measured immediately after its preparation. The fresh mango puree obtained was adjusted to 3 levels of TSS (20, 22 and 24 °B) by adding analytical grade sucrose and three levels of acid content (0.50, 0.56 and 0.62 g/100 g) in terms of citric acid) by adding

analytical grade citric acid, and the effect of TSS and acid content was observed on following parameters.

### **3.2.6.2 Water activity**

The water activity of the sample was measured by water activity meter (aqua lab, USA, Dew Point 4TE). Before the sample analysis, the equipment was calibrated with the calibration kit provided with the equipment.

### **3.2.6.3 Back extrusion**

The back extrusion test is based on the displacement of the material through an annular gap between probe and the container. As the probe is lowered the material is pressed up through the annular gap, whereas when the probe is raised the material flows back through the annular gap into the cell. The force is measured in the down and up cycle at a defined position. The back extrusion test of the sample was carried out by following the method of Alkarkhi et al. [2] with some modifications using Texture Analyzer (Stable Micro Systems, UK, TA HD plus) with supporting Exponent Lite software. The container supplied with the equipment was filled up to the 75 % of the height with the sample. When a surface trigger of  $49.05 \times 10^{-3}$  N was attained (i.e. the point at which the probe's lower surface is in full contact with the product), the disc proceeds to penetrate to a depth of 30 mm with a test speed of 1 mm/s followed by returning to the original position. The force vs distance plot generated was used to obtain the following parameter:

1. Firmness: The peak or maximum force is taken as a measurement of firmness.
2. Consistency: The area of the curve up to this peak is taken as a measurement of consistency.
3. Cohesiveness: The maximum negative force during the return of the probe is taken as an indication of the cohesiveness.
4. Work of cohesion: The area of the negative region of the curve may be referred to as the 'work of cohesion.

### **3.2.6.4 Dynamic rheology**

The method of Gundurao et al. [11] with minor modifications was followed for dynamic rheology study. A controlled-stress rheometer (Anton Paar, Austria, MCR 72) equipped with a manufacturer supplied computer control software was used to study dynamic oscillatory measurement. The test was carried out with a shear rate of 1 % and at

a frequency sweep from 0.1 to 10 Hz. A 50-mm parallel plate attachment was used with a gap of 0.5 mm. For each test, approximately 2 mL sample was placed on the bottom plate of the rheometer and the separate test was conducted at 30 and 90 °C. The exposed sample perimeter was enclosed with a plastic trap to minimize evaporation at a higher temperature.

### 3.2.6.5 Differential Scanning Calorimetry (DSC) and Thermo-gravimetric Analysis (TGA)

The DSC and TGA of the mango puree samples were performed to evaluate the variations in thermal behavior and temperature-mass relationship respectively. About 9 mg of the isolated compound was placed in a silica crucible for analysis of the thermal properties of the compound using simultaneous thermal analyzer (NETSCH, Germany, STA 449F3 Jupiter). The argon gas was purged continuously at a flow rate of 1ml/min over a temperature range of 25 to 175 °C, with a constant heating rate of 10 °C/min.

### 3.2.6.6 Ohmic heating profile

The OH was carried out in a lab scale set up as discussed in section 3.1. The mango puree samples with different TSS and acid content were heated at four, 10, 20, 30 and 40 V/cm EFS. The samples were heated from ambient conditions ( $27 \pm 2$  °C) and the heating process was stopped once the temperature at the centre of the material reached  $90 \pm 1$  °C.

### 3.2.7 Optimization of ohmic heating process parameters

Three variable factorial design of response surface methodology was used for the optimization of the OH process parameters for mango puree processing. The details of the dependent and independent variables are listed in Table 3.5. The experimental design and optimization was conducted using Design Expert © software version 7.0.0 (Stat-Ease, Inc. 2021 East Hennepin Ave, Suite 480 Minneapolis, MN 55413).

**Table 3.4 Process variable for optimization of ohmic heating process**

S No.	Independent variables			Levels	Dependent variables
	Variable	Unit	Unit		
1	Electric strength	field	$V.cm^{-1}$	15, 20 and 25	PPO and POD Residual activity Bacterial count (CFU/mL)
2	Temperature		°C	85, 90 and 95	Color change ( $\Delta E$ )
3	Time		min	1, 1.5 and 2	

### 3.2.8 Parameters measured for the optimization process

#### 3.2.8.1 Poly-phenol oxidase (PPO) essay

PPO activity was determined according to Charles et al. [7], one gm of sample and 25 mL of 0.1 M sodium phosphate buffer (pH 6.5) were mixed together using vortex shaker followed by centrifugation (Sigma, Germany, 3-18K) at  $1.3 \times 10^4$  rpm at 4 °C for 20 min. The reaction mixture containing 0.5 ml enzyme extract, 2.2 mL of 0.05 M sodium phosphate buffer (pH 6.5) and 0.8 mL of substrate 0.1 M solution catechol (double distilled water as blank) was incubated at  $30 \pm 1$  °C for 30 min. Finally, the reaction was stopped by heating the mixture at in boiling water for 10 min and the PPO activity was assayed by measuring absorbance at 395 nm by UV-Vis spectrophotometer (Cecil Instruments, England, CE 7400).

#### 3.2.8.2 Peroxidase (POD) essay

POD activity was measured by the method of Brochier et al. [6], the extract of enzyme was made by mixing 1:4 parts of mango puree and of 0.05 M phosphate buffer pH 7.0 with the help of vortex shaker for 1.5-2 min. Further the mixture was centrifuged (Sigma 3-18K, Germany) at  $6 \times 10^3$  rpm for 10 min while maintaining temperature at 4 °C followed by filtration using normal filter paper. For the determination of POD activity the absorbance of a mixture of 1.5 mL of 0.1 M phosphate buffer (pH 5.0) 1 mL of the extract, 0.2 mL of 1% hydrogen peroxide solution and 0.5 mL of 1.5 % guaiacol (or 0.5 mL of double distilled water for blank) was measured at 460 nm using spectrophotometer (Cecil Instruments CE 7400, England).

The change in absorbance was recorded an interval of 10 s for 4 min. One unit of PPO or POD activity is defined as the amount of enzyme causing 0.01 absorbance change per min. Linear part of the absorption curve was taken into account and the enzyme activity was measured from the slope as depicted in Fig 3.4.

#### 3.2.8.3 Bacterial count estimation

The bacterial Count was estimated according to the method of Naresh et al. [19]. The decimal diluted sample serially with sterile 1 mg/mL peptone water and appropriate dilutions was poured on to the respective plates. Plate count agar was used for determination of bacterial counts (BC) and then plates were incubated at 37 °C for 48–72 h. The microbial counts were expressed as colony forming units every ml of the sample (CFU/mL)

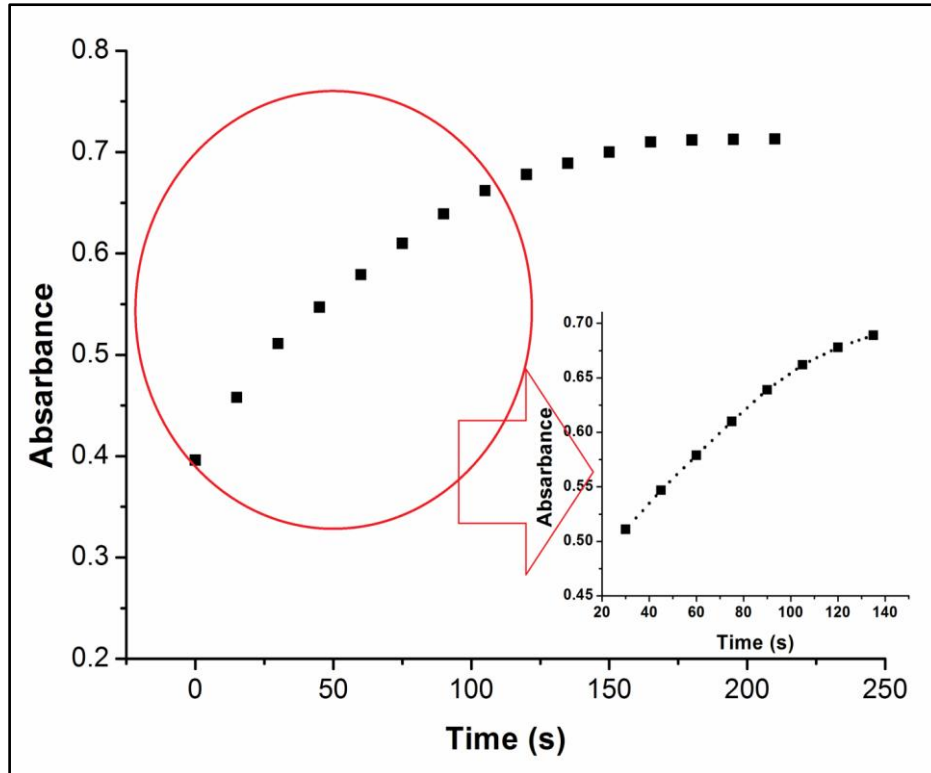


**Fig. 3.4** Depiction of enzyme activity calculation

#### 3.2.8.4 Color measurement and Color change ( $\Delta E$ )

CIE (Internationale de l'éclairage) color parameters  $L^*$  (lightness);  $a^*$  (red–green) and  $b^*$  (yellow–blue) of the samples was estimated using a Hunter color Lab (Ultra-Scan VIS, Hunter Lab, USA). The parameters were further used to calculate the color change ( $\Delta E$ ) as reported by Kaushik et al. [17] using Eq. 3.14.

$$\text{Total color difference } \Delta E^* = [(\Delta L^*)^2 + (\Delta a^*)^2 + (\Delta b^*)^2]^{1/2} \quad \text{Eq. (3.14)}$$

#### 3.2.9 Enzymes and microbial inactivation kinetics modeling

The kinetics study for the enzymes (PPO and POD) inactivation was fitted with the six different models listed as Eq. 3.15 to Eq. 3.20 Brochier et al. [6]. Whereas the bacterial reduction and change in color ( $\Delta E$ ) was fitted with the exponential and linear model using Eq. 3.23 and Eq. 3.24, respectively. The best fit model for the above parameters was selected on the base of the least Chi square (Eq. 3.25) and highest determination coefficient ( $R^2$ ) value. The models and equations used in present study are briefly described as follows.



### 3.2.9.1 First order reaction

The enzyme inactivation is assumed to be a one-step irreversible, and the assumption is that breaking of a single bond or a structure is sufficient to inactivate the enzyme. The expression for the model is as Eq. 3.15.

$$\frac{A_t}{A_0} = \exp(-k \cdot t) \quad \text{Eq. (3.15)}$$

### 3.2.9.2 Distinct isozymes

This model describes that the inactivation takes place by the sum of two exponential decays, one for thermo labile enzyme and another for thermo resistant enzyme [8]. The expression for the model is Eq. 3.16.

$$\frac{A_t}{A_0} = A_L \cdot \exp(-k_L \cdot t) + A_R \cdot \exp(-k_R \cdot t) \quad \text{Eq. (3.16)}$$

### 3.2.9.3 Two-fraction

The two-fraction describes that plant material contain a variety of isozymes that can be categorized into two groups, one having higher resistance to heat than the other more. And both follow first order during inactivation due to heat [8] as mentioned in Eq. 3.17.

$$\frac{A_t}{A_0} = a \cdot \exp(-k_L \cdot t) + (1 - a) \cdot \exp(-k_H \cdot t) \quad \text{Eq. (3.17)}$$

### 3.2.9.4 Fractional conversion

This model (Eq.3.18) defines the inactivation by first order while takes into account the non-zero activity ( $A_r$ ), due to the presence of heat resistant fraction. The expression of the model is mentioned in Eq. 3.18 and ' $A_r$ ' is activity attained at the equilibrium [24].

$$\frac{A_t}{A_0} = A_r + (A_0 - A_r) \cdot \exp(-k \cdot t) \quad \text{Eq. (3.18)}$$

### 3.2.9.5 Weibull distribution

The Weibull distribution expressed as Eq.3.19, suggests a continuing degradation of the enzyme and it is illustrated by two factors 'b' and 'n'. The value of 'n' and 'b' describes the shape of the curve and the thermal reduction rate respectively; hence 'n' is called as the shape factor whereas the 'b' is known as the scale factor [12].

$$\frac{A_t}{A_0} = \exp(-b \cdot t^n) \quad \text{Eq. (3.19)}$$

### 3.2.9.6 n<sup>th</sup> order

The n<sup>th</sup> order model (Eq. 3.20) is a general model where the value of ‘n’ describes the concavity of the plot. The value  $n < 1$  and  $n > 1$  indicates the upward and downward concavity, respectively [27].

$$\frac{A_t}{A_0} = [A_0^{1-n} + (n - 1).kt]^{\left(\frac{1}{n-1}\right)} \quad \text{Eq. (3.20)}$$

Where

$A_0$	Initial enzyme activity	$A_t$	Enzyme activity at time ‘t’
$K$	Rate constant	$t$	time
$k_l$	Rate constant of labile fraction	$k_r$	Rate constant of resistant fraction
$A_r$	Activity at equilibrium	$b$	Scale factor
$n$	Shape factor		

### 3.2.9.7 Decimal reduction time (D-value)

The time required reducing the activity or population by 1-log cycle at a specific temperature is known as D-value and was calculated using the Eq. 3.21.

$$\text{D-value} = \frac{2.303}{k} \quad \text{Eq. (3.21)}$$

Where ‘k’ is the rate constant.

### 3.2.9.8 Thermal resistance constant (Z-value)

The change in temperature required to cause 1 log reduction in the D value is known as Z value. It was calculated using the Eq. 3.22.

$$\text{Z-value} = \frac{T_2 - T_1}{\text{Log}\left(\frac{D_1}{D_2}\right)} \quad \text{Eq. (3.22)}$$

Where  $T_1$  and  $T_2$  is lower and higher temperature respectively and  $D_1$  and  $D_2$  are the respective D value at  $T_1$  and  $T_2$ .

### 3.2.9.9 Exponential model for bacterial reduction

The first order exponential reduction is expressed as Eq. 3.23.

$$\frac{N_t}{N_0} = \exp^{-kt} \quad \text{Eq. (3.23)}$$

Where, ‘ $N_t$ ’ and ‘ $N_0$ ’ is number of colonies at heating time ‘t’, and at  $t=0$  (without treatment) respectively and ‘k’ is the reduction rate constant.

### 3.2.9.10 Temperature dependency of bacterial inactivation

The activation energy ( $\text{kJ}\cdot\text{mol}^{-1}\cdot\text{K}^{-1}$ ) was calculated from the Arrhenius equation (Eq. 3.24).

$$\ln \frac{k_2}{k_1} = -\frac{E_a}{R} \left( \frac{1}{T_2} - \frac{1}{T_1} \right) \quad \text{Eq. (3.24)}$$

Where  $k_1$  and  $k_2$  are the reduction rate constant at temperature  $T_2$  and  $T_1$  respectively,  $E_a$  is the activation energy and 'R' is the universal gas constant ( $8.314 \text{ J/mol/K}$ ).

### 3.2.9.11 Linear model for color change ( $\Delta E$ )

$$\Delta E = mt + \Delta E_0 \quad \text{Eq. (3.25)}$$

Where, ' $\Delta E$ ' and ' $\Delta E_0$ ' is change in color at time 't' and '0' respectively and m '' is the slope of the linearity.

### 3.2.9.12 Chi-square ( $\chi^2$ ) value

$$\chi^2 = \sum \frac{(A_p - A_e)^2}{n - p} \quad \text{Eq. (3.26)}$$

Where ' $A_p$ ' and ' $A_e$ ' is predicted and experimental residual activity respectively, 'n' is the number of observations and 'p' is the number of parameters.

### 3.2.10 Effects of ohmic heating process on mango puree and its storage behavior

The mango puree was treated with optimized OH conditions and evaluated to estimate the effects of OH processing on various parameters of mango puree. To compare the effects of OH process with conventional heating method, another parallel sample was heated by hot water (HW) method (using a water bath). The heating profile of the HW water treatment was maintained to be same as that of OH process.

Additional aim of this objective was to evaluate the effects of Come-up-Time (CUT) or heating time separate samples were heated up to the desired temperature i.e.  $95^\circ\text{C}$  by both OH and HW method without heating further rather immediately cooled down using chilled water. Whereas, for checking effect of holding time the samples were heated up to  $95^\circ\text{C}$  and kept for 115 s at the temperature, followed by immediate cooling using chilled water. The coding and conditions of the treatment are mentioned in Table 3.6. The OH and HW treated (optimized condition) samples were stored at ambient temperature ( $25\pm 2^\circ\text{C}$ ) in pre-sterilized  $30\pm 1 \text{ ml}$  glass vials (Borosil) as shown in Fig. 3.5. The storage

study was conducted for 3-months and the samples were withdrawn and analyzed at an interval of 15 days.

**Table 3.5 The sample coding for OH and HW treatment studies**

<b>Treatment</b>	<b>Treatment conditions</b>
Control	With no treatment
OH-0	Heating up to 95 °C by OH method at 15 V/cm
HW-0	Heating up to 95 °C by HW method
OH-115	Heating up to 95 °C and holding for 115 sec at 95 °C by OH method at 15 V/cm
HW-115	Heating up to 95 °C and holding for 115 sec at 95 °C by HW method

### 3.2.10.1 Hot water or conventional heat treatment (HW)

The conventional thermal processing of mango pulp was performed using the water bath (BW-20G, JEIOtech, Korea). To compare the effects of OH and HW heating the samples were treated in closed tubes for same time and similar temperature histories as that of optimized OH conditions (95 °C for 108 s).

The OH and HW treatment of mango puree was compared by evaluating following parameters after treatment and during storage.

### 3.2.10.2 TSS, Titratable acidity, pH, and TBC

TSS, Titratable acidity, pH and BC were determined following the method mentioned as in section 3.2.4.3-4.5 and 3.2.8.4 respectively.

### 3.2.10.3 Steady shear flow behavior

The method of Ahmed et al. [1] was used for conduct the flow behavior with small modification. Rheometer (Anton Paar, MC200 SN310475) equipped with a manufacturer supplied computer control software was used to study the effects of the treatment (OH and HW) on the flow characteristics of mango puree. The test was conducted using cone and plate assembly of 50-mm diameter and 2° angle. Approximately 3 mL of sample was placed on the bottom plate and the test was conducted while maintain a gap of 1 mm between the cone and plate. The shear rate was varied in between 0.01 and 200/s and the test were performed at 25 °C (room temperature).

### 3.2.10.4 Modeling flow behavior of mango puree

The steady shear flow behavior of mango puree after the treatment and during storage was analyzed for various models listed in Table 3.7. The models were selected on the

basis of recommendations of Ahmed et al. [1]. The best fit model was selected on the basis of least root mean square error (RMSE) and highest coefficient of determination ( $R^2$ )

**Table 3.6 List of the models analyzed for steady shear flow behavior of mango puree**

S. No	Model	Equation	Equation no
1.	Newtonian	$\sigma = k(\gamma)$	Eq. (3.29)
2.	Power	$\sigma = k(\gamma)^n$	Eq. (3.30)
3.	Casson	$\sigma = [k_0 + k(\gamma)^{0.5}]^2$	Eq. (3.31)
4.	Bingham	$\sigma = \sigma_0 + k(\gamma)$	Eq. (3.32)
5.	Herschel–Bulkley	$\sigma = \sigma_0 + k\gamma^n$	Eq. (3.33)

Where:

$\sigma$ Shear stress (Pa)	$\sigma_0$ Yield stress (Pa)	k Consistency coefficient (Pa.sn)
n Flow behavior index	$\gamma$ Shear rate (s <sup>-1</sup> )	k <sub>0</sub> Constant consistency factor

### 3.2.10.5 Extraction of particle phase (cell wall material)

The separation of particle phase from the serum phase of mango puree was carried out by following the method of Jamsazzadeh et al. [16]. Approximately 10 mL of the puree was centrifuged (Sigma 3-18K, Germany) for 60 min at  $10.5 \times 10^3$  g at room temperature, the serum phase (supernatant) was discarded and the pellet was again twice centrifuged with 10 mL double distilled water for 15 min to wash away any residual serum present. The wet pellet was dried in vacuum oven (560 mm Hg) at 50 °C for 12-14 hours. Finally the dry cell wall material was stored in air sealed pouches for morphological studies.

### 3.2.10.6 Scanning Electron Microscopy (SEM)

Scanning Electron Microscopy (SEM) instrument (JSM-6390 LV, Japan, PN junction type, semiconductor detector) was used to obtain the micrograms of the cell wall material of Control, OH and HW treated mango puree. The 1000X images were captured using 20 kV accelerating potential.

### 3.2.10.7 Vitamin C

The Vitamin C content was estimated by modified method of Watada et al. [28]. Five grams of sample were added into 25 mL meta-phosphoric acid solution (20 %) and the final volume was made to 100 mL by double distilled water. Titration of 10 mL aliquot of volume made was carried with 0.05 % (w/v) 2, 6 dichloroindophenol dye solution. The titration was stopped when light pink color persisted for 15 s and the

volume of dye consumed was measured. Standardization of pure ascorbic acid was carried out by AOAC [4] method and Vitamin C content in sample was calculated from the Eq. 3.28.

$$\text{Ascorbic acid (mg/100g)} = \frac{\text{Titer value of sample} \times \text{dye factor} \times \text{volume made up} \times 100}{\text{aliquot taken for estimation} \times \text{sample weight}} \quad \text{Eq. (3.28)}$$

### 3.2.10.8 Total phenolic content (TPC)

The total phenolic content (TPC) was determined by spectrophotometer method using Gallic acid as standard, according to the method described by the Anesini et al. [3]. One ml of the sample was transferred in tubes containing 5.0 ml of a of Folin-Ciocalteu's reagent solution (1:10 dilution), followed by adding 4 ml of sodium carbonate solution (7.5 % w/v). The tubes were then allowed to stand at room temperature for 1 hour before the measurement of absorbance at 765 nm against water. The TPC are expressed as mg Gallic acid equivalents (GAE) per 100 g sample. The concentration of total phenols was derived from a standard curve of Gallic acid ranging from 0 to 200  $\mu\text{g/L}$  (Fig. 3.6).

### 3.2.10.9 $\beta$ -carotenes

The total  $\beta$ -carotene content was estimated by following the method of Nagata and Yamashita [18]. One gram of sample was added into 10 mL of 4:6 (v/v) acetone and hexane solution. The mixture was homogenized at  $16 \times 10^3$  rpm for 1 min followed by the light absorption measurement at wavelength of 663, 645, 505, and 453 nm using UV Vis spectrophotometer. The  $\beta$ -carotenoids were calculated by Eq. 3.27 and expressed as mg/100 mL.



Fig. 3.5 Samples stored in glass vials

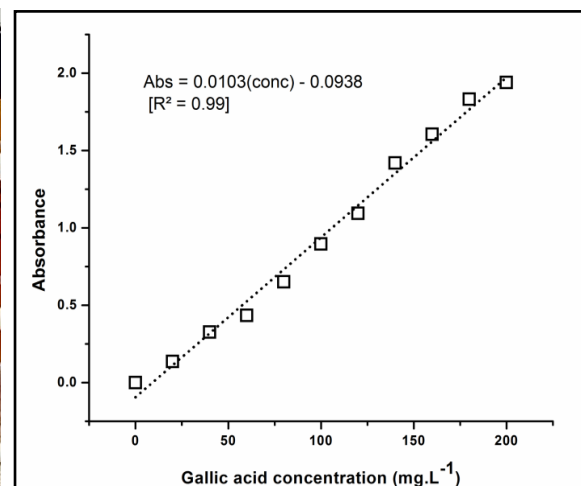


Fig. 3.6 Standard curve of gallic acid

$$\begin{aligned} \beta - \text{carotene (mg/100 mL)} & \qquad \qquad \qquad \text{Eq. (3.27)} \\ & = 0.216 A_{663} - 1.22 A_{645} - 0.304 A_{505} + 0.452 A_{453} \end{aligned}$$

### **3.2.11 Statistical Analysis**

Statistical analysis for the data was performed using SPSS (Statistical Package for the Social Sciences) software version 16.0. Analysis of Variance (ANOVA) and Duncan's multiple range tests were carried out on the observed data at 95 % confidence level ( $p < 0.05$ ). And the kinetic modeling was performed using Origin Pro 8.5 software and Microsoft Excel 2007. Significance tests were carried out at 95 % confidence interval using Duncan's multiple range tests ( $p < 0.05$ ).

**References**

- [1] Ahmed, J., Ramaswamy, H. S., and Hiremath, N. The effect of high-pressure treatment on rheological characteristics and colour of mango pulp. *International Journal of Food Science and Technology*, 40, 885-895, 2005.
- [2] Alkarkhi, A. F., bin Ramli, S., Yong, Y. S. and Easa, A. M. Comparing physicochemical properties of banana pulp and peel flours prepared from green and ripe fruits. *Food Chemistry*, 129(2): 312-318, 2011.
- [3] Anesini, C., Ferraro, G. E., Filip, R. Total polyphenol content and antioxidant capacity of commercially available tea (*Camellia sinensis*) in Argentina. *Journal of Agricultural and Food Chemistry*, 56(19), 9225-9229, 2008
- [4] AOAC; Official Methods of Analysis (13th edition) Association of Official Analytical Chemists, Washington, DC, 1985.
- [5] Bozkurt, H., and Icier, F. Exergetic performance analysis of ohmic cooking process. *Journal of Food Engineering*, 100(4), 688-695, 2010.
- [6] Brochier, B., Mercali, G. D., and Marczak, L. D. F. Influence of moderate electric field on inactivation kinetics of peroxidase and polyphenol oxidase and on phenolic compounds of sugarcane juice treated by ohmic heating. *LWT - Food Science and Technology*, 74, 396-403, 2016.
- [7] Charles, F., Vidal, V., Olive, F., Filgueiras, H. and Sallanon, H. Pulsed light treatment as new method to maintain physical and nutritional quality of fresh-cut mangoes. *Innovative Food Science and Emerging Technologies*, 18, 190-195, 2013.
- [8] Chen, C. S., and Wu, M. C. Kinetic models for thermal inactivation of multiple pectinesterases in citrus juices. *Journal of Food Science*, 63(5), 747-750, 1998.
- [9] Darvishi, H., Hosainpour, A., Nargesi, F., Khoshtaghaza, M. H. and Torang, H. Ohmic Processing: Temperature Dependent Electrical Conductivities of Lemon Juice. *Modern Applied Science*, 5(1), 209-216, 2011.
- [10] Ghnimi, S., Flach-malaspina, N., Dresch, M., Delaplace, G., and Maingonnat, J. F. Design and performance evaluation of an ohmic heating. *Chemical Engineering Research and Design*, 86, 626-632, 2008
- [11] Gundurao, A., Ramaswamy, H. S., and Ahmed, J. Effect of Soluble Solids Concentration and Temperature on Thermo-Physical and Rheological Properties of Mango Puree. *International Journal of Food Properties*, 14, 1018-1036, 2011.
- [12] Hutchinson, T. P. Graphing the death of *Escherichia coli*. *International Journal of Food Microbiology*, 62(1-2), 77-81, 2000.
- [13] Icier, F., and Ilicali, C. Temperature dependent electrical conductivities of fruit purees during ohmic heating. *Food Research International*, 38, 1135-1142, 2005.
- [14] Icier, F., and Ilicali, C. The effects of concentration on electrical conductivity of orange juice concentrates during ohmic heating. *European Food Research and Technology*, 220, 406-414, 2005.



- [15] Icier, F., Colak, N., Erbay, Z., Kuzgunkaya, E. H., and Hepbasli, A. A Comparative Study on Exergetic Performance Assessment for Drying of Broccoli Florets in Three Different Drying Systems. *Drying Technology*, 28(2), 193-204, 2010.
- [16] Jamsazzadeh Kermani, Z., Shpigelman, A., Bernaerts, T. M. M., Van Loey, A. M., and Hendrickx, M. E. The effect of exogenous enzymes and mechanical treatment on mango purée: Effect on the molecular properties of pectic substances. *Food Hydrocolloids*, 50, 193-202, 2015.
- [17] Kaushik, N., Kaur, B. P., Rao, P. S., and Mishra, H. N. Effect of high-pressure processing on color, biochemical and microbiological characteristics of mango pulp (*Mangifera indica* cv. Amrapali). *Innovative Food Science and Emerging Technologies*, 22: 40-50, 2014.
- [18] Nagata, M., and Yamashita, I. Simple method for simultaneous determination of chlorophyll and carotenoids in tomato fruit. *Nippon Shokuhin Kogyo Gakkaishi*, 39(10), 925-928, 1992.
- [19] Naresh, K., Varakumar, S., Variyar, P. S., Sharma, A. and Reddy, O. V. S. Effect of  $\gamma$ -irradiation on physico-chemical and microbiological properties of mango (*Mangifera indica* L.) juice from eight Indian cultivars. *Food Bioscience*, 12: 1-9, 2015.
- [20] Nguyen, L. T., Choi, W., Lee, S. H., and Jun, S. Exploring the heating patterns of multiphase foods in a continuous flow, simultaneous microwave and ohmic combination heater. *Journal of Food Engineering*, 116, 65-71, 2013.
- [21] Nicholson, J. W. *The Chemistry of Polymers* (4, Revised ed.). Royal Society of Chemistry. 2011
- [22] Olivera, D. F., Salvadori, V. O. and Marra, F. Ohmic treatment of fresh foods: Effect on textural properties. *International Food Research Journal*, 20(4): 1617-1621, 2013.
- [23] Pereira, R. N., Rodrigues, R. M., Genisheva, Z., Oliveira, H., de Freitas, V., Teixeira, J. A., and Vicente, A. A. Effects of ohmic heating on extraction of food-grade phytochemicals from colored potato. *LWT - Food Science and Technology*, 74, 493-503, 2016.
- [24] Rizvi, A. F., and Tong, C. H. Fractional conversion for determining texture degradation kinetics of vegetables. *Journal of Food Science*, 62(1), 1-7, 1997.
- [25] Samaranayake, C. P., and Sastry, S. K. Effects of controlled-frequency moderate electric fields on pectin methylesterase and polygalacturonase activities in tomato homogenate. *Food Chemistry*, 199, 265-272, 2016.
- [26] Sarang, S., Sastry, S. K., and Knipe, L. Electrical conductivity of fruits and meats during ohmic heating. *Journal of Food Engineering*, 87(3), 351-356, 2008.
- [27] Saxena, J., Makroo, H. A., Bhattacharya, S., and Srivastava, B. Kinetics of the inactivation of polyphenol oxidase and formation of reducing sugars in sugarcane juice during Ohmic and conventional heating. *Journal of Food Process Engineering*, 41(3), e12671, 2017.
- [28] Watada, A. E., Aulenbach, B. B. and Worthington, J. T. Vitamins A and C in ripe tomatoes as affected by stage of ripeness at harvest and by supplementary ethylene. *Journal of Food Science*, 41(4): 856-858, 1976.